World Journal of Advanced Engineering Technology and Sciences
eISSN: 2582-8266
Cross Ref DOI: 10.30574/wjaets
Journal homepage: https://wjaets.com/

(RESEARCH ARTICLE)

Check for updates

Robust-PID controller design for magnetic levitation system using parameter space approach

Moayed Almobaied *, Hassan S. Al-Nahhal and Khaled B.A. Issa

Department Electrical Engineering, Islamic University of Gaza, Gaza, Palestine.

World Journal of Advanced Engineering Technology and Sciences, 2023, 08(02), 135–151

Publication history: Received on 07 February 2023; revised on 15 March 2023; accepted on 18 March 2023

Article DOI: https://doi.org/10.30574/wjaets.2023.8.2.0084

Abstract

Recently, implementation of air magnetic suspension systems has become more challenging due to the growing demand for lightweight technologies, comfortable cabins, vehicle safety stability, and pollution control. Magnetic levitation, or Maglev, is the method of propelling a target into the air by adjusting different magnetic forces. The absence of contact and the avoidance of wear and friction phenomena are key considerations in the applications of magnetic levitation technology. Due to the high nonlinearity in the modelling process of such kind of systems, the stabilizing of magnetic levitation has been considered as a challenging task for many researchers in control engineering sector. The computation of all stabilizing PID gains controllers for the magnetic levitation benchmark ED-4810 (Maglev) is demonstrated in this paper using two different scenarios. In the first one, the tuning parameters of the classical PID controller (KP, KI, and KD) are assumed to be the uncertain parameters. The second scenario demonstrates the uncertainty in the transfer function of the system by using the resistance and the inductance as uncertain parameters. The characteristic polynomial of the linearized uncertain model is shown to be an unstable affine polynomial using the Zero Exclusion Theorem and the singular frequencies technique. The parameter space approach is used to illustrate the values of all PID parameters in order to achieve robust stability in the two scenarios. The effectiveness of the presented graphical technique has been verified through MATLAB simulation to obtain robust stability for magnetic levitation systems.

Keywords: Linearized model; Proportional–integral–derivative controller (PID); Robust control system; Characteristic polynomial; Singular frequency.

1 Introduction

Magnetic Levitation (Maglev) is the technique of suspending an object in the air by adjusting magnetic force which is used to counteract the gravitational force of the object [1]. The magnetic levitation technique is a widely advanced and expanding technology where the common feature in their applications is the absence of contact, which means no wear and friction. This enhances performance, lowers maintenance costs, and extends the system's life cycle [2]. The Maglev process have recently been implemented in a variety of industries such as: transportation, commercial applications, small and big wind turbines, and clean energy[3]. Vehicles that move like trains along a guideway using magnets to generate both lift and propulsion are important practical examples where frictions have been reduced to a great extent level which results in extremely high velocities [4]. Such systems' mathematical models have high nonlinearity and are unstable. Therefore, there is a significant need for research on modelling and controlling magnetic levitation systems in academic institutions and research centres. The linear system model and the nonlinear model are two well-known classification strategies for analysing systems that can be seen in the literature. For the linearized model: Proportional Integral control (PI), proportional–integral–derivative control (PID), Fuzzy logic controller, and linear–quadratic regulator (LQR) approaches are commonly applied as in [5-8]. According to [5], a magnetic levitation system (MLS) is a highly nonlinear open loop system which can be controlled by a proportional integral derivative (PID) controller with

* Corresponding author: Moayed Almobaied

a derivative filter coefficient. The graphic PID development methodology for the maglev system was published in [9], which used the D-partition approach in the design of controller. Sliding mode control, Lyapunov functions, and output feedback control are a promising techniques for nonlinear viewpoints [10-12]. Although PID is the easiest and most inexpensive of these controllers in develop and implement, the major drawback of PID controller is a tuning of PID gains (KP, KI, and KD). There are numerous ways to adjust the PID controller's parameters. The following are many examples of these popular strategies: the Z-N (Ziegler-Nichols) approach[13], Integral of Squared time weighted Error (ISE) method[14], Cohen-Coon methodology[15], Integral of Absolute Error rule (IAE)[16], and technique of gain-phase margin[17].

Actually, the suggested controller's robustness in the existence of parameter variation in the system is not taken into account by either of the abovementioned traditional processes. The study of complex systems with uncertainties is one of the most significant subfields of robust control. The characteristic polynomials for any uncertain systems include one or more uncertain parameters as the algebraic variables of its characteristic equation. There are different forms of polynomial families: polynomial coefficients, affine linear coefficients, multilinear coefficients, and interval coefficients. The classification is dependent on how uncertain parameters are included in the polynomial coefficients [18]. The ED-4810 magnetic levitation system's resulting characteristic polynomial in this study is an affine structure where the uncertain variables enter the characteristic polynomial coefficients linearly. There are numerous effective techniques used in control research literature for verifying the stability of specific plants. However, conventional approaches such as the Routh-Hurwitz standard and Root Locus are difficult to function in the presence of uncertainty. The Zero Exclusion Principle procedure is an effective tool for testing stability in an affine parameter space[19-21].

In [22] The authors use the parameter space strategy to calculate all stabilizing PID parameters (KP, KI, and KD) for the magnetic levitation ED-4810 system with parametric uncertainties. The authors of this article apply the parameter space technique to modify parameters of the classical PID controller (KP, KI, and KD) that are considered to be uncertain parameters. The remainder of this article is structured as follows. The mathematical modelling of ED-4810 magnetic levitation and problem formulation are introduced in Section II. Section III defines the stability test approaches for uncertain architectures. The suggested robust PID controller is constructed and the collection of all PID stabilizing areas is recognized in section IV. section V's discussion of the simulation results. Finally, section VI includes final observations.

2 Magnetic Levitation Modelling System

Fig. 1 depicts the ED-4810 magnetic levitation system model which confirms the magnetic levitation principle of a suspended steel ball in the air with magnetic force. Because of the high nonlinearity in its model, this system is suitable for testing the effectiveness of different kinds of controllers in university laboratories [18].

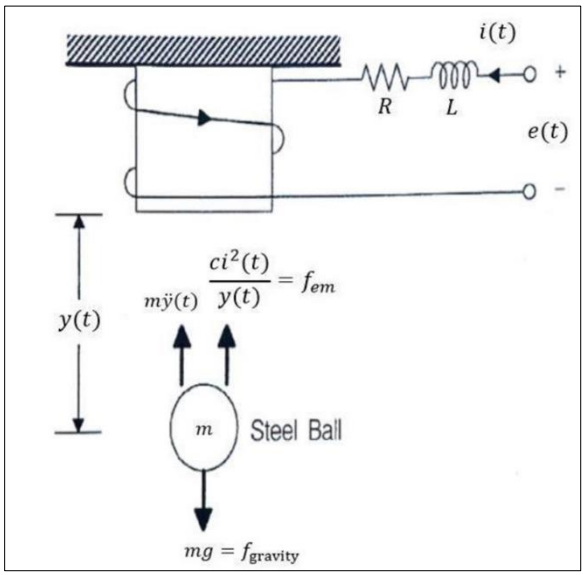

Figure 1 Magnetic levitation system model

Where:

m: The steel ball's weight.
y(t): The ball's position in the middle.
i(t): An electromagnetic coil is experiencing an electric current.
c: The strength of magnetism.
L: A wire's inductance.
R: The wire's resistance.
e(t) is the input voltage.

Equation (1) shows the mathematical relation between the coil's current and its voltage.

$$e(t) = Ri(t) + L\frac{di(t)}{dt} \text{.....(1)}$$

The combined value of the force applied on the perpendicular as shown in Fig. 1 is as follows:

$$f_{total} = f_{gravity} + f_{em} \text{.....(2)}$$

Where the magnetic force of the top coil is commonly denoted f_{em}, and $f_{gravity}$ is the weight of gravity. The first order differential formulas listed below serve as a representation of the mathematical model of the actual system shown in Fig. 1.

$$m\ddot{Y} = mg - c\frac{i^2}{y} \text{.....(3)}$$

$$\dot{x}_a = x_b \text{.....(4)}$$

$$\dot{x}_b = g - \frac{cx_c^2(t)}{mx_a} \text{.....(5)}$$

$$\dot{x}_c = -\frac{R}{L}i_c + \frac{1}{L}u(t) \text{.....(6)}$$

Where, $x_a \triangleq y(t), x_b \triangleq \dot{y}, x_c \triangleq i(t), u(t) \triangleq e(t)$.

It is clear that the derived state formulas are nonlinear. As a result, these formulas need to be linearized in order to employ the proposed methodology.

The linearization procedure will take into account the following presumptions.

- $x_a = x_1 = y^*$, where x_1 is the ball's distance and y^* is the ball's center of equilibrium.
- $x_b = x_2 = 0$ is represented as the ball's speed.
- The ball's acceleration is represented by the equation $\dot{x}_b = 0$.
- the current $i(t)$ is defined as is $x_c = x_3$ and $\dot{x}_c = 0$.

As a result, equation 3 can be used to determine the value of x_c as follows:

$$x_c = x_3 = i^* = \sqrt{\frac{mgy^*}{c}} \text{.....(7)}$$

The common linearization techniques have been described by [23]. The final linearized state-space model is specified by the following equation:

$$\begin{bmatrix} \dot{x}_a \\ \dot{x}_b \\ \dot{x}_c \end{bmatrix} = \begin{bmatrix} 0 & 1 & 0 \\ \frac{g}{y^*} & 0 & \frac{-2}{y^*}\sqrt{\frac{cg}{m}} \\ 0 & 0 & -\frac{R}{L} \end{bmatrix} \begin{bmatrix} x_a \\ x_b \\ x_c \end{bmatrix} + \begin{bmatrix} 0 \\ 0 \\ \frac{1}{L} \end{bmatrix} u(t) \text{.....(8)}$$

$$y(t) = [1 \quad 0 \quad 0]\begin{bmatrix} x_a \\ x_b \\ x_c \end{bmatrix} \text{.....(9)}$$

The resulting transfer function of the linear system model is:

$$G(s) = \frac{\sqrt{\frac{4ycg}{m}}}{-LyS^3 - RyS^2 + LgS + gR} \text{.....(10)}$$

R and L were both chosen as the uncertain variables in this investigation. Table 1 shows the values of the other constants.

The transfer function will be as follows by replacing the values in equation 10 from table 1:

$$G(s) = \frac{42}{-3LS^3 - 3RS^2 + 980LS + 980R} \text{..... (11)}$$

Table 1 Specific ED-4810 magnetically levitated system specifications and their values [23]

Parameters	**Values**	**Units**
m	2	2Kg
g	9.8	m/s^2
c	0.3	-
y^*	0.03	m
i^*	1.44	A

The transfer function's characteristic polynomial in equation 11 is:

$$P(S, R, L) = -3LS^3 - 3RS^2 + 980LS + 980R \text{.....(12)}$$

The aforementioned polynomial family falls within the category of affine polynomials, where the polynomial components are linearly entered by the uncertain variables R and L so that $R \in [45,55]$, $L \in [0.15,0.25]$. In robust theory the uncertain quantities are represented by the letter q i.e: $q_1 \triangleq R$, $q_2 \triangleq L$. As a result, we may rewrite the characteristic equation as:

$$P(S, q_1, q_2) = -3q_2S^3 - 3q_1S^2 + 980q_2S + 980q_1 \text{.....(13)}$$

3 Stability Test

An important consideration in control system theory is stability. The stability of linear plants can be tested for specific systems using numerous well-known techniques, such the Routh-Hurwitz, Root locus, and Nyquist plot, among others. However, it's likely that these strategies won't work if the system model has uncertainties. Actually, it is hard to quickly and generally determine whether a particular uncertain system is stable or not. For special circumstances, there are many different techniques and theorems that can be useful. Singular frequencies and the Zero Exclusion Theorem are effective methods for assessing the stability of affine polynomial families. The system is considered robustly stable if and only if all component of the value set of the system represented by uncertain parameters is stable. [18]. The parameter box is the collection of all possible values for a parameter vector created from interval parameters. Fig. 2 in this study illustrates the parameter box for the two uncertain variables mentioned in the preceding section.

3.1 Zero Exclusion Theorem

The affine polynomial family is robustly stable if and only if the value set of the polynomial family excludes the origin for every $\omega > 0$, according to the concept of Zero Exclusion Theorem. The polynomial family's value set at a certain frequency is defined as:

$$P(j\omega.Q) \triangleq [P_c(j\omega, q) \in c | q \in Q] \text{.....(14)}$$

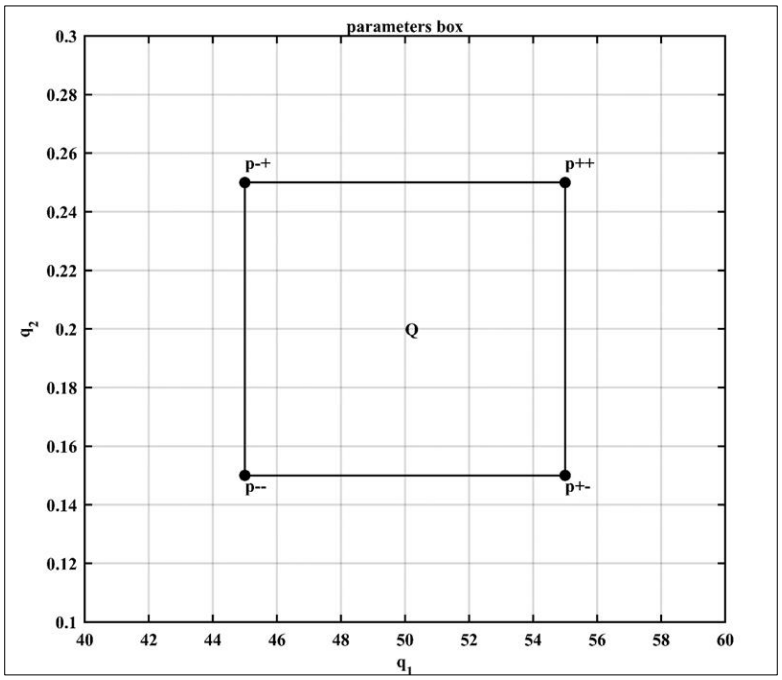

Figure 2 Parameter box for the ED-4810 system

There is at least one value for ω in unstable systems in which the origin is shown on the value set graph (pole at $j\omega$). When the crossover to the imaginary axis only occurred place at a single frequency. It is challenging to show that the polynomial series is unstable by manually gridding the imaginary poles and applying the Zero Exclusion Principle to all resulting candidate singular frequencies. Singular frequencies should therefore be carefully investigated as candidate frequency for instability tests. However, the Jacobi approach can be used to find singularity of frequencies as illustrated below [21]:

To begin, the original polynomial family $P(S, q_1, q_2)$ is divided into even and odd polynomials as follows:

$$P(j\omega, q)_{even} = -3q_1\omega^2 + 980q_1 \text{.....(15)}$$

$$P(j\omega, q)_{odd} = -3q_2\omega^3 + 980q_2\omega \text{.....(16)}$$

The Jacobian matrix $J(\omega, q)$ can be defined as:

$$J(\omega, q) \triangleq \begin{bmatrix} \frac{dP(j\omega,q)even}{dq_1} & \frac{dP(j\omega,q)even}{dq_2} \\ \frac{dP(j\omega,q)odd}{dq_1} & \frac{dP(j\omega,q)odd}{dq_2} \end{bmatrix} \text{.....(17)}$$

Accordingly, using equations 15 and 16, the polynomial family's resulting Jacobian matrix can be created as follows:

$$J(\omega, q) = \begin{bmatrix} -3\omega^2 + 980 & 0 \\ 0 & -3\omega^3 + 980\omega \end{bmatrix} \text{.....(18)}$$

When the determinant of J(ω,q) vanishes, the singularity occurs:

$$|J(\omega, q)| = (-3\omega^3 + 980\omega)(-3\omega^2 + 980) = 0 \text{.....(19)}$$

The candidate singular frequencies obtained by solving equation 19 are: $\omega_{s1} = 0$, $\omega_{s2} = -\sqrt{980/3}$, $\omega_{s3} = -\sqrt{980/3}$, $\omega_{s4} = \sqrt{980/3}$, and $\omega_{s5} = \sqrt{980/3}$. Neglect is established of the two negative frequencies, ω_{s2} and ω_{s3}. For $\omega_{s1} = 0$, the second condition is violated $p(0,q)_{even} = 980q_1 \neq 0$. Hence, this candidate frequency $\omega_{s1} = 0$ is not singular frequency. By graphing, Fig. 3 shows that the $\omega_{s1} = 0$ candidate singular frequency which excludes the origin at this frequency is not singular.

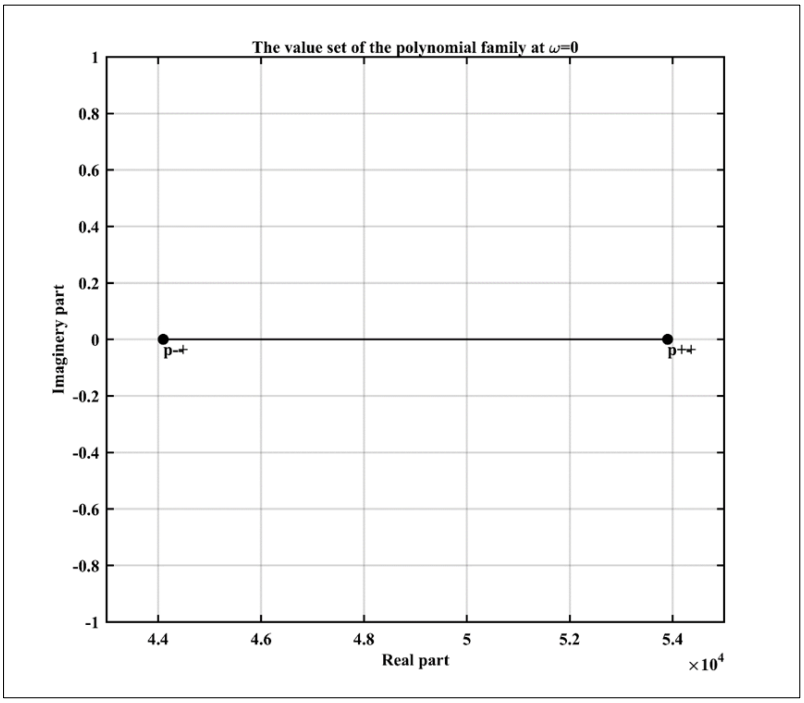

Figure 3 Value set at ω_s1=0

For $\omega_{s4,5} = \sqrt{980/3}$, The 2nd and 3rd prerequisites have both been fulfilled. i.e $p(\sqrt{980/3}, q)_{odd} = 0$ and $p(\sqrt{980/3}, q)_{even} = 0$. Hence, $\omega_{s4,5} = \sqrt{980/3}$ are replicated points with singular frequencies. Actively planning the polynomial's value set at this frequency demonstrates the statistical evidence for this assertion., which includes the origin which is shown by Fig. 4.

The Mikhailov plot is depicted by Fig. 5, in which the value set of the polynomial series for $0 < \omega < 20$ rad/sec is conveyed. Based on the Zero Exclusion Principle and vanishing frequency technique, the polynomial combination in equation 13 is hence unstable.

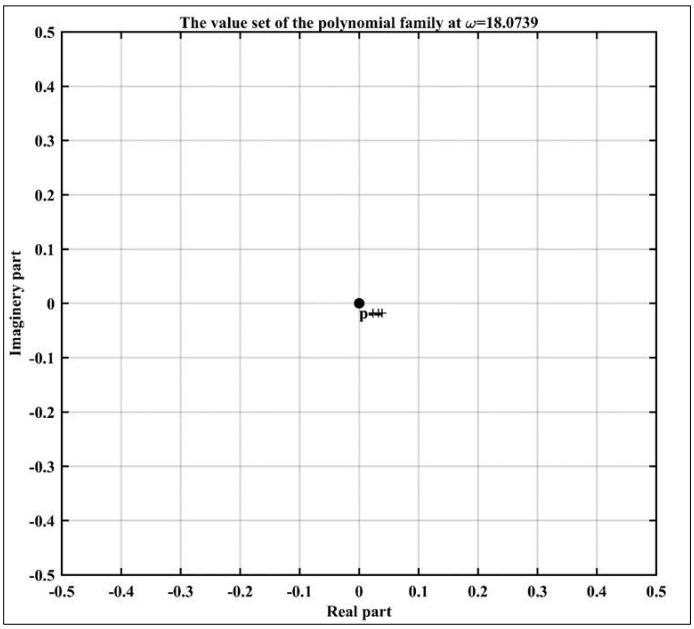

Figure 4 Value set at $\boldsymbol{\omega_{s4,5}} = \sqrt{\frac{\mathbf{980}}{\mathbf{3}}}$

4 Robust PID Controller Design

PID controllers have been tuned using a variety of methods, such as the Ziegler-Nichols and Nyquist approaches. However by adopting these conventional methods, the developers will only obtain a single collection of (K_P, K_I, and K_D) design variables. However, the parameter space methodology provides a graphical strategy that can be used to find all PID stability zones and is regarded as a vital tool for challenging robust stability. Equation 20 displays the open - loop system unknown transfer function that was generated in equation 11 except with q_1, q_2 in instead of R and L for resistor and inductor , respectfully.

$$G(s) = \frac{42}{-3q_2s^3 - 3q_1s^2 + 980q_2s + 980q_1} \dots\dots\dots\dots (20)$$

Where,$q_1 \in [45,55]$, $q_2 \in [0.15,0.25]$.

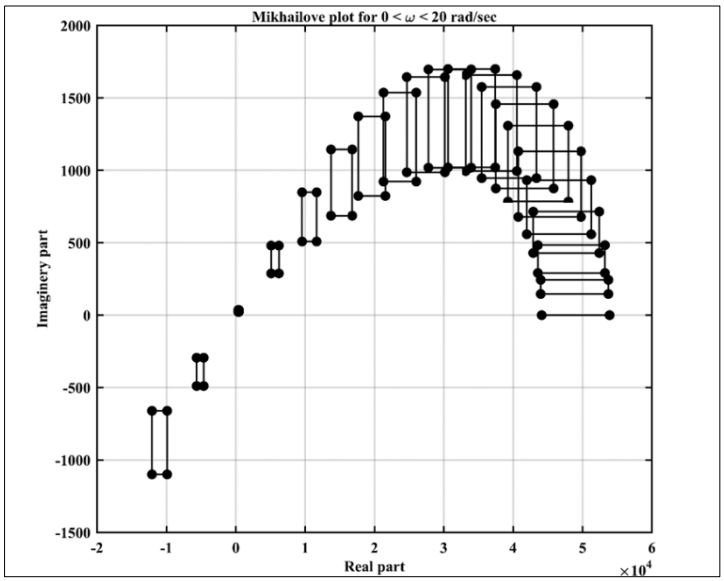

Figure 5 Plot of Mikhailov for 0<ω<20 rad/sec

The following is the transfer function for the conventional PID controller:

$$G(s) = \frac{K_D S^2 + K_P S + K_I}{S} \text{.....(21)}$$

The open - loop system transfer function for the magnetic levitation system. when R and L are selected 50Ω and $0.2H$ respectively is:

$$G(s) = \frac{-70}{S^3 + 250S^2 - 326.67S - 81666.67} \text{ ..... (22)}$$

Fig. 6 shows the closed-loop with PID controller for the electromagnetic levitation system. If the PID parameter blocks have the following values: $K_P = -2018$, $K_D = -250$ and $K_I = -45180$. They have been obtained through a number of trials in order to obtain the good results. Fig. 7 demonstrated the step response for the system when this PID controller is used. However, this PID controller is established at the nominal values of the uncertain parameters $R = 50\Omega$ and $L = 0.2H$, but if this values are change into $R = 55\Omega$ and $L = 0.25H$ the system will be unstable as shown in Fig. 8. As a result, it has been demonstrated that this controller is not robust. In fact, a PID controller is considered a robust controller when it guarantees system stability for all values of uncertain parameters. This is lead to use the parameter space approach in the two following subsections to determine all PID parameter stability areas which is regarded as a wonderful instrument for sturdy stabilizing challenges.

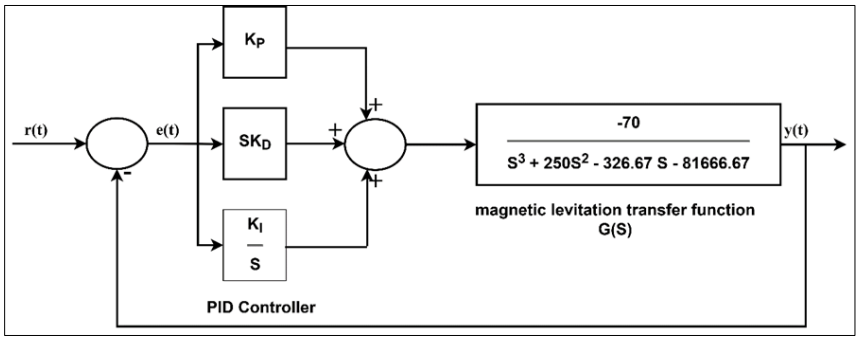

Figure 6 The closed-loop PID control of the magnetically levitated device

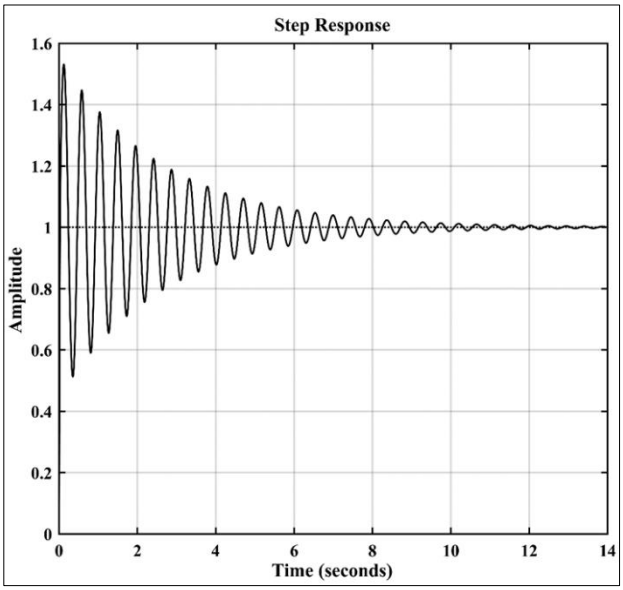

Figure 7 The magnetic levitation system's step response using a PID controller at nominal values for the uncertain parameters R=50Ω and L=0.2H

4.1 Hurwitz Stabilizing PID Controller

The closed-loop control scheme for the linear system is shown in Fig. 6. 50Ω and $0.2H$ are chosen for R and L, respectively. The polynomial with closed - loop system characteristics is so as follows:

$$P(S, K_D, K_P, K_I) = -3S^4 - 750S^3 + (210\mathrm{K_D} + 980)S^2 + (210K_P + 245000)S + 210K_I \ldots\ldots (23)$$

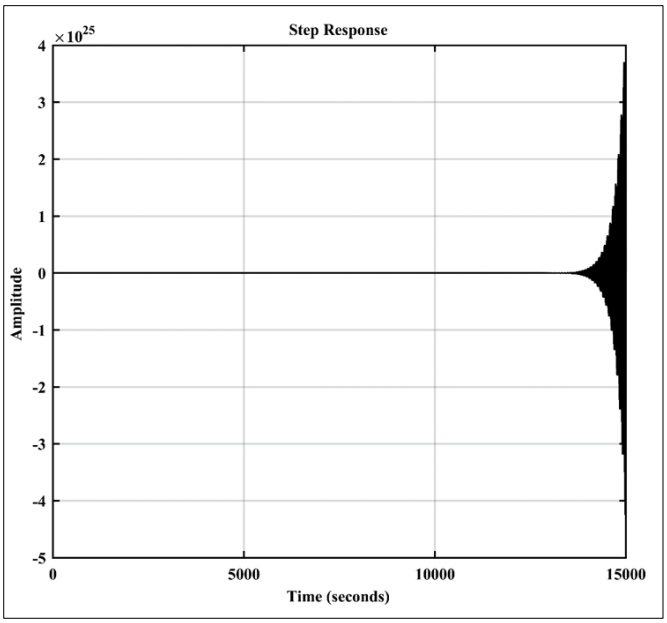

Figure 8 The magnetic levitation system's step response using a PID controller at nominal values for the uncertain parameters R=55Ω and L=0.25H

In the mapping of the stability border to the variables space, the parameter space technique may be used to discover the stability zones in the space [18]. For $P(S, K_D, K_P, K_I)$ the real and imaginary components are:

$$Real = 210K_I - 210\omega^2 K_D - 3\omega^4 - 980\omega^2 \ldots\ldots\ldots\ldots (24)$$

$$Img = 750\omega^3 + (245000 + 210K_P)\omega \ldots\ldots\ldots\ldots\ldots\ldots (25)$$

The matrix representation of equations (24) and (25) is described as the following:

$$\begin{bmatrix} 210 & -210\omega^2 \\ 0 & 0 \end{bmatrix} \begin{bmatrix} K_I \\ K_D \end{bmatrix} + \begin{bmatrix} -3\omega^4 - 980\omega^2 \\ 750\omega^3 + (245000 + 210K_p)\omega \end{bmatrix} = 0 \ldots\ldots\ldots (26)$$

The parameter space methodology performs well enough when only two factors are being assessed. Another solution for displaying stabilization zones when there are more than two factors in the dimensional space is to reset all factors other than two. There is a particular instance of PID control system where it is simple to establish that the stabilization zones for a specific K_P quantity have polygon pattern[18]. The formulation of equation 26 is $Ax + b = 0$ which is straightforward. The determinant of A matrix should not exceed 0 in sequence to have a solution. The determinant of A matrix in this scenario is:

$$Det(A) = \begin{vmatrix} 210 & -210\omega^2 \\ 0 & 0 \end{vmatrix} \ldots\ldots\ldots\ldots (27)$$

The aforementioned determinant drops for any ω. As a consequence, in equations 24 and 25, K_I and K_D's graphically solutions seem to be either equivalent or parallel curves in the parametric plane instead of a point. The definition of the parameter K_P must be declared inside a range in order to preserve similarity between the two curves.

$$\frac{0}{210} = \frac{0}{210\omega^2} = \frac{750\omega^3 + (245000 + 210K_P)\omega}{-3\omega^4 - 980\omega^2} \ldots\ldots\ldots\ldots (28)$$

Then,

$$\omega^2 = -\frac{245000 + 210K_P}{750} \ldots\ldots\ldots\ldots (29)$$

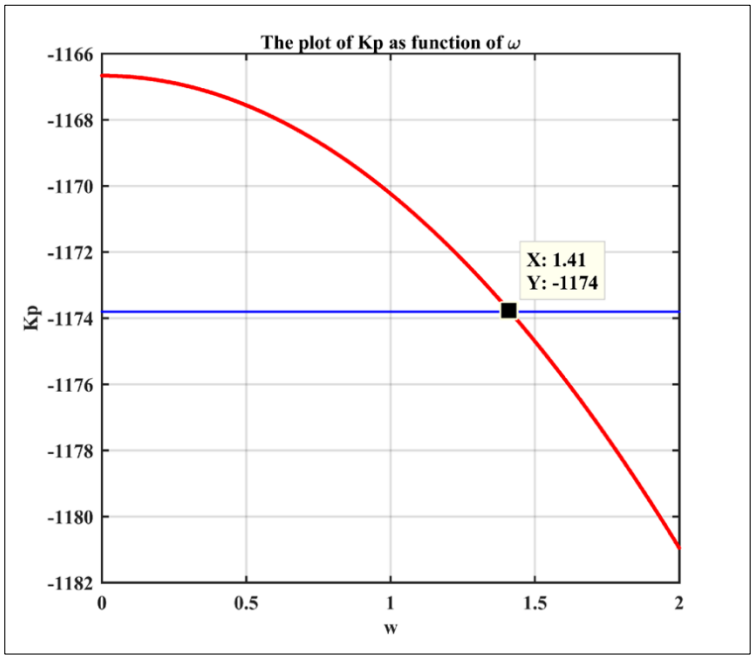

Figure 9 Kp as function of ω for P(s)

Considering that the frequencies have to be higher than zero, the K_p is chosen to provide the result $(245000 + 210K_P) \leq 0$. The requirement to guarantee the similarity of the curves in equations 24 and 25 is $K_P < -1166.7$. When $K_P = -1173.8$ is utilized, the value of ω is equal to $\sqrt{2}$, as shown in equation 29 or Fig. 9, which graphically illustrates the link between K_P and ω.

By adjusting the K_P quantity in equations 24 and 25 we get:

$$Real = 210K_I - 210\omega^2 K_D - 3\omega^4 - 980\omega^2 \ldots\ldots\ldots\ldots (30)$$

$$Img = 750\omega^3 - 1500\omega \ldots\ldots\ldots\ldots (31)$$

Fig. 10 exemplifies the stability zones of both K_I and K_D for $P(s)$ where: (RRB) Real root boundary at $\omega = 0$ is $K_I = 0$, (IRB) Infinity root boundary at $\omega = \infty$ does not exist, and (CRB) Complex root boundary at $\omega = \sqrt{2}$:

$$210K_I - 420K_D = 1972 \ldots\ldots\ldots\ldots (32)$$

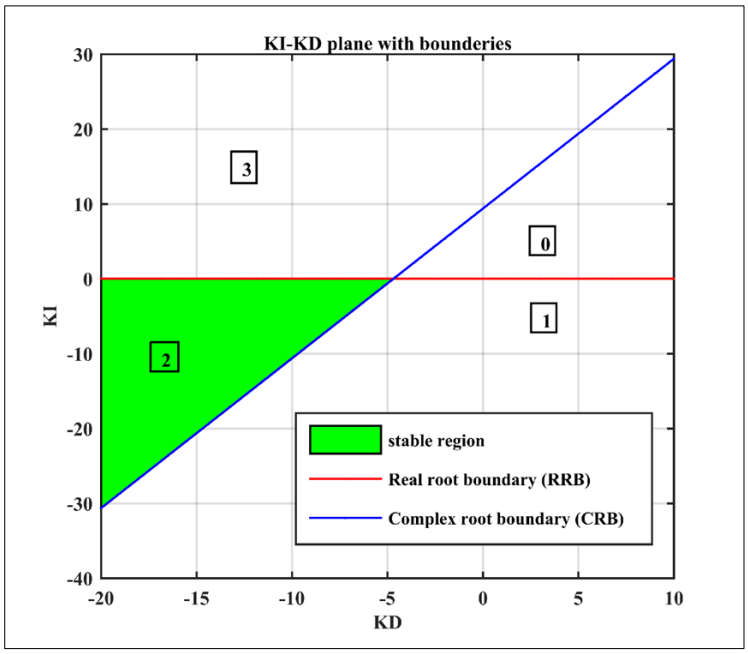

Figure 10 $K_I - K_D$ plane for $P(s)$

The plot is divided into four discrete sections by curves in Fig. 10. According to the Boundary Crossing Principle, when any of these zones has a stable equation, then the remainder of the zone must also contain stable polynomials. The polynomials in the other zones must likewise be unstable if one of these zones contains an unstable polynomial. As a consequence, by selecting single polynomial and confirming its stability for each region, the collection of stability zones may be fully described. There is only one stable zone is evident when this approach is used on the graph in Fig. 10.

4.2 Robust Stabilization PID Controller

The closed - loop control scheme for the indeterminate electromagnetic levitation system where R and L are undefined variables is shown by Fig. 11. Thus, the following is the characteristic equation:

$$P(S, q_1, q_2) = -3q_2S^4 - 3q_1S^3 + (980q_2 + 42K_D)S^2 + (980q_1 + 42K_P)S + 42K_I \ldots\ldots (33)$$

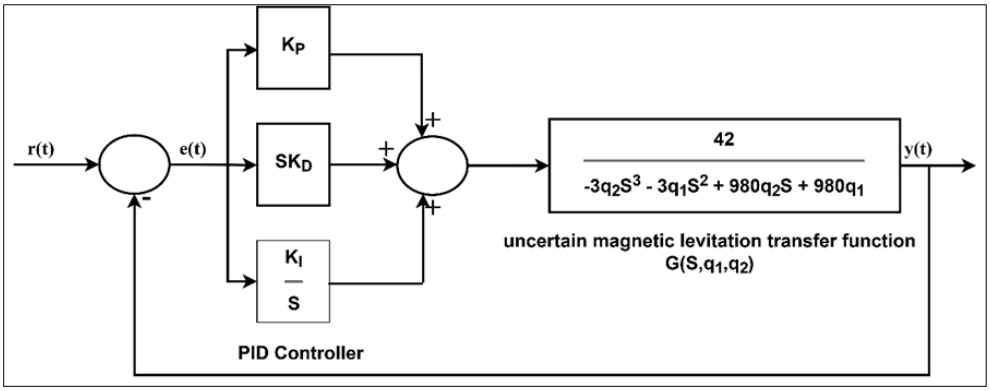

Figure 11 The looped Control scheme of the uncertain electromagnetic levitation system

To use Khartinov's argument for stability, the polynomial series should belong to the interval category[21]. The coefficients may be over limited in the affine polynomial transformation to interval. This could be performed by assuming that the affine polynomial's variables are independent[18]. This strategy works despite being a little conservative. Exactly two polynomials need to be checked to guarantee stability in the sense of Khartinov's argument because the closed - loop system polynomial series in equation 33 is of degree 4. [18]:

$$P^{+-} = a_0^+ + a_1^- S + a_2^- S^2 + a_3^+ S^3 + a_4^+ S^4 \ldots\ldots\ldots\ldots(34)$$

$$P^{++} = a_0^+ + a_1^+ S + a_2^- S^2 + a_3^- S^3 + a_4^+ S^4 \ldots\ldots\ldots\ldots\ldots(35)$$

In equations 34 and 35, the required parameters can be used to find the necessary polynomials to evaluate the stability:

$$P^{+-} = -0.45S^4 - 135S^3 + (147 + 42K_D)S^2 + (44100 + 42K_D)S + 42K_I \ldots\ldots\ldots\ldots(36)$$

$$P^{++} = -0.45S^4 - 165S^3 + (147 + 42K_D)S^2 + 43900 + 42K_P)S + 42K_I \ldots\ldots\ldots\ldots(37)$$

To discover the stability areas for the two aforementioned polynomials the procedure of parameter space is employed. For P^{+-} the real and imaginary components are:

$$P_{Real}^{+-} = -0.45\omega^4 - (147 + 42K_D)\omega^2 + 42K_I \ldots\ldots(38)$$

$$P_{Img}^{+-} = 135\omega^3 + (44100 + 42K_P)\omega \ldots\ldots\ldots\ldots\ldots(39)$$

The matrix representation of the two equations previously is described as the following:

$$\begin{bmatrix} 42 & -42\omega^4 \\ 0 & 0 \end{bmatrix} \begin{bmatrix} K_I \\ K_D \end{bmatrix} + \begin{bmatrix} -0.45\omega^4 - 147\omega^2 \\ 135\omega^3 + (44100 + 42K_p)\omega \end{bmatrix} = 0 \ldots\ldots\ldots(40)$$

Instead of a point in equations 38 and 39, K_I and K_D 's graphical solutions are either identical in the parameter plane or parallel lines. The K_P parameter's must be set within a varies so that the two lines' symmetry can be guaranteed.

$$\frac{0}{42} = \frac{0}{42\omega^2} = \frac{135\omega^3 + (44100 + 42K_P)\omega}{-0.45\omega^4 - 147\omega^2} \ldots\ldots\ldots\ldots \quad (41)$$

Then,

$$\omega^2 = -\frac{44100 + 42K_P}{135} \ldots\ldots\ldots(42)$$

The actually gets of K_P is $(44100 + 42K_P) \leq 0$. The need to guarantee the identical of the curves in equations 38 and 39 is indeed $K_P < -1050$. According to equations 42 or Fig. 12 which graphically illustrates the connection between K_P and ω. The value of ω is comparable to 35.1 when $K_P = -5000$.

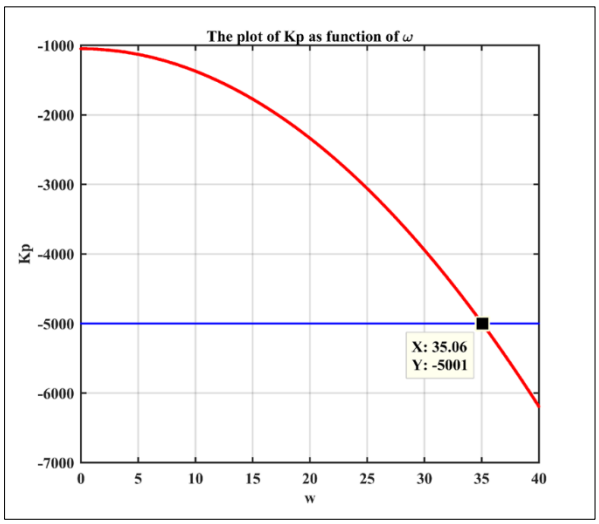

Figure 12 K_P as function of ω for P+-

By Changing the value of K_P in equations 38 and 39, we obtain:

$$P_{Real}^{+-} = -0.45\omega^4 - (147 + 42K_D)\omega^2 + 42K_I \text{.....(43)}$$

$$P_{Img}^{+-} = 135\omega^3 - 2160\omega \text{.....(44)}$$

Figure 13 demonstrates the stable zones of both k_I and K_D for P^{+-} for P(+-): (RRB) Real root boundary at $\omega = 0$ is $K_I = 0$, (IRB) Infinity root boundary at $\omega = \infty$ does not exist , and (CRB) Complex root boundary at $\omega = 35.1$:

$$42K_I - 51744.42K_D = 864137.36 \text{.....(45)}$$

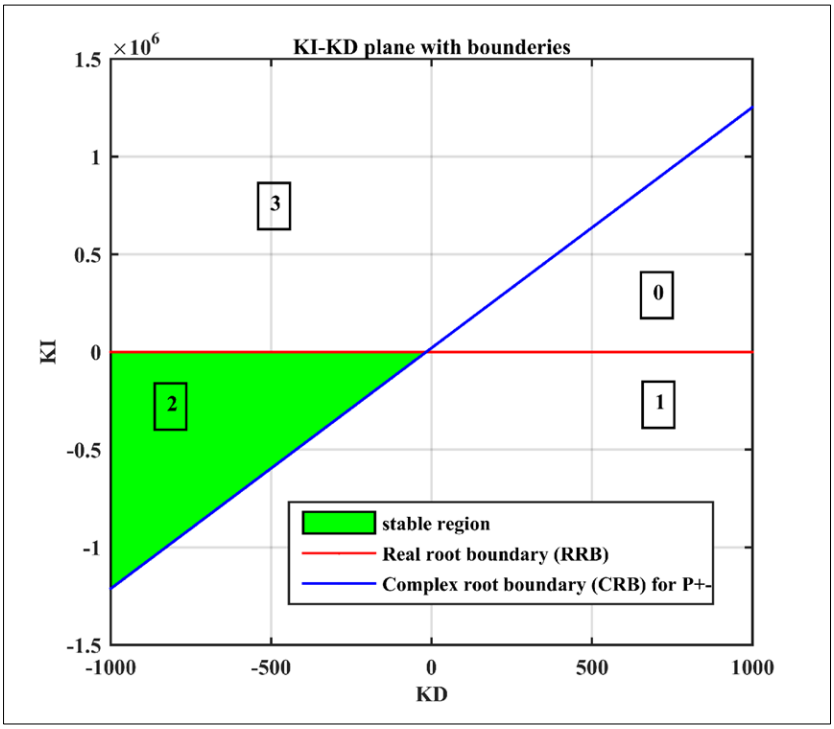

Figure 13 K_I and K_D Plane for P^{+-}

The graph in Fig. 13 illustrates one stable zone. The steps described above ought to be repeated for the P^{++} family of polynomials where:

$$P_{Real}^{++} = -0.45\omega^4 - (147 + 42K_D)\omega^2 + 42K_I \text{ ... ...(46)}$$

$$P_{Img}^{++} = 165\omega^3 + (43900 + 42K_P)\omega \text{.....(47)}$$

These two equations have a matrix form:

$$\begin{bmatrix} 42 & -42\omega^4 \\ 0 & 0 \end{bmatrix} \begin{bmatrix} K_I \\ K_D \end{bmatrix} + \begin{bmatrix} -0.45\omega^4 - 147\omega^2 \\ 165\omega^3 + (43900 + 42K_P)\omega \end{bmatrix} = 0 \text{..... (48)}$$

Fig. 14 exemplifies the relationship K_P with ω For both P^{++} and P^{+-}. For P^{++}, K_P should have a magnitude less than -1045. As a result, we picked $K_P = -5000$ as the quantity of K_P to satisfy both P^{++} and P^{+-} conditions, with the resulting ω for P^{++} equivalent to 31.77. Hence, by altering the magnitude of K_P as follows, equations 46 and 47 can be restructured:

$$P_{Real}^{++} = -0.45\omega^4 - (147 + 42K_D)\omega^2 + 42K_I \text{.....(49)}$$

$$P_{Img}^{++} = 165\omega^3 - 2360\omega \text{.....(50)}$$

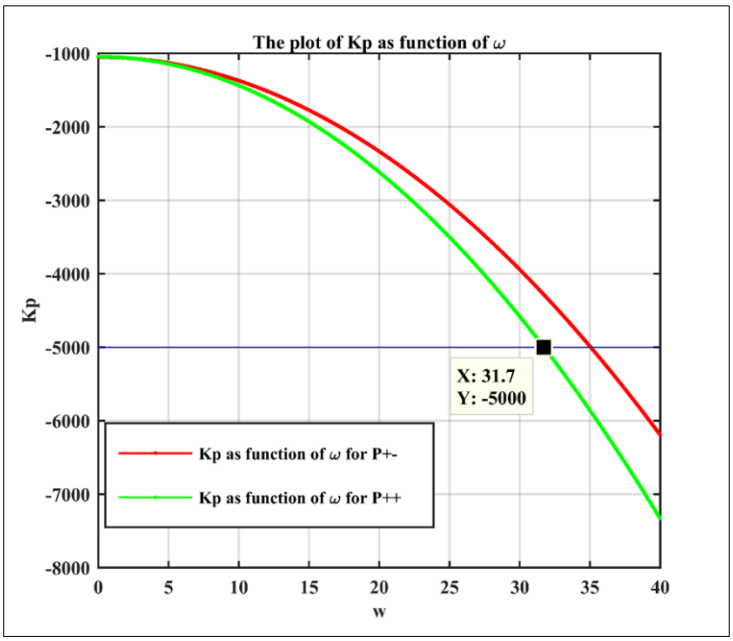

Figure 14 $\boldsymbol{K_P}$ as function of ω for both $\boldsymbol{P^{++}}$ and $\boldsymbol{P^{+-}}$

The Stability zones of K_I and K_D for P^{++} are depicted in Fig. 15 where: (RRB) Real root boundary at $\omega = 0$ is $K_I = 0$, (IRB) Infinity root boundary at $\omega = \infty$ does not exist, and (CRB) Complex root boundary at $\omega = 31.77$:

$$42K_I - 42391.98K_D = 606810.74 \text{.....(51)}$$

As can be seen in Fig. 15, the "$K_I - K_D$" space was split into four new sections by the P^{++} RRB and CRB curves. As a result, it is possible to locate the stable zone of P^{++} in the same manner as in the earlier scenario. By comparing the stability zones for P^{+-} and P^{++} in Fig.16 we can conclude that the stability zone for P^{++} is a subset of the one for P^{+-}. As a result, the stability region of P^{++} ensures the stability zone for the system polynomial family .

5 Results and Simulation

The preceding section outlined the necessary tasks to identify every region of trying to stabilize PID gain parameters for the ED-4810 magnetic levitation system with parametric uncertainties. To ensure that the results are stable, we will select many sites inside these zones in this phase. For instance, if the given point is picked beyond the stabilization zones: $K_P = -1174, K_I = 1, K_D = 1, q_1 = 50\Omega$ and $q_2 = 0.2h$ then the characteristic equation that results will now be $p(s) = (-3S^4 - 750S^3 + 1190S^2 - 1500S + 210)$ which is unstable in the sense of the conventional Routh–Hurwitz technique to examine the stability. However, if we pick any values for PID parameters that are inside the stable range, the system that results will be stable for any variables inside of the provided regions: $45 < q_1 = R < 55$ and $0.15 < q_2 = L < 0.25$.

Table 2 compares the performance of the given system when $K_P = -5000, K_I = -8000$, and $K_D = -850$ are selected as well as different values for uncertain parameters. Performance is shown in terms of overshot, rising time, settling time, and peak time. Because the all PID parameters are negative, their values can be inverted by placing an inverting operational amplifier to modify the negative values of the PID parameters $[K_p, K_d, K_i]$ into positive values.

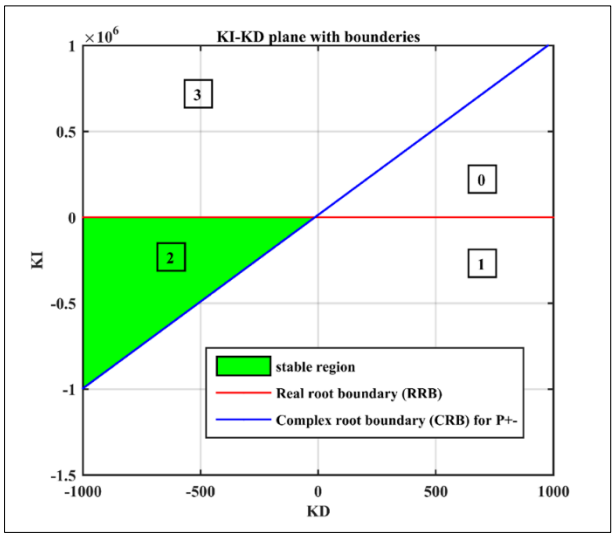

Figure 15 K_I and K_D Plane for P^{++}

Table 2 Response values for $K_P = -5000, K_I = -8000,$ and $K_D = -850$

Uncertain Parameters Values	Tr (sec)	Tp (sec)	O.S %	Ts (sec)
q1 = 45Ω, q2 = 0.15h	0.006	0.014	20	1.21
q1 = 48Ω, q2 = 0.2h	0.007	0.016	23.6	1.21
q1 = 50Ω, q2 = 0.18h	0.006	0.316	21	1.21
q1 = 50Ω, q2 = 0.2h	0.007	0.016	22.1	1.21
q1 = 52Ω, q2 = 0.22h	0.007	0.016	22.6	1.21
q1 = 45Ω, q2 = 0.25h	0.007	0.016	31.3	1.21

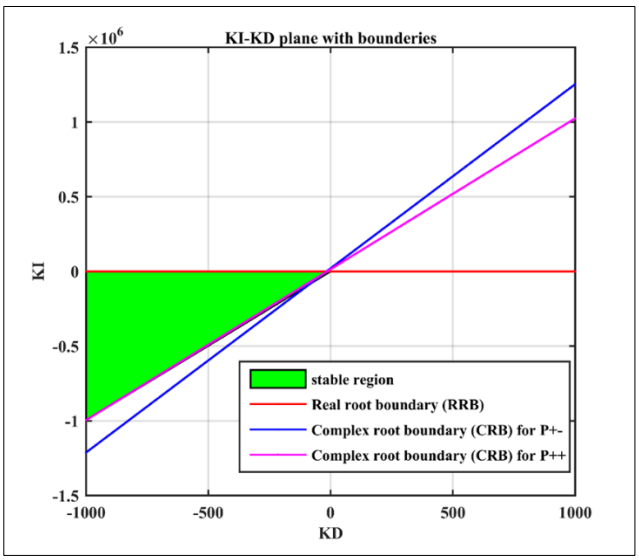

Figure 16 K_I and K_D Plane for P^{+-} and P^{++}

Furthermore, Fig. 17 shows sample step responses for various PID Parameter values within the stability range as well as various locations within the specified parametric uncertainty bounds q_1 and q_2.

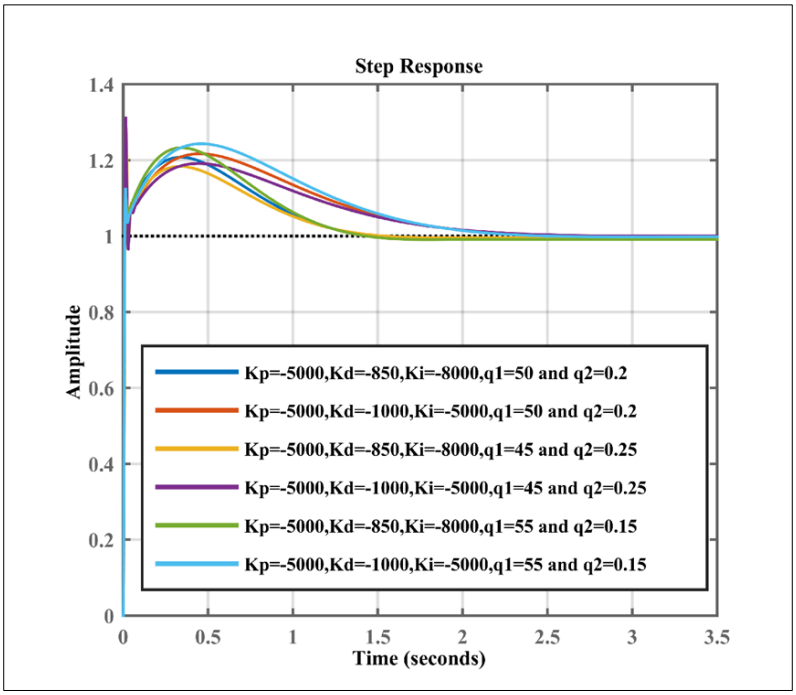

Figure 17 Step Response of Maglev for various PID Parameter Values

6 Conclusion

In this research, two scenarios were used to estimate all stabilization PID gains for the ED-4810 magnetically levitated system (Maglev). The tuning parameters of the classical PID controller (KP, KI, and KD) which are considered to be uncertain parameters is demonstrated by first scenario. The second scenario illustrates the uncertainty in the system's transfer function by using resistance and inductance as uncertain parameters. The Zero Exclusion Principle (ZET) and the singular frequencies methodology are first used to investigate the stability of the uncertain open-loop system and it is observed that the corresponding polynomial series has an unstable affine structure. All stabilizing PID parameter ranges are then established using the graphical parameter space technique. The outcomes of the MATLAB simulation demonstrate the flexibility in choosing the stabilization PID gains that generate a robustly stable ED-4810 magnetically levitated system with parameter variation in both R and L. When the PID gains are chosen to be within this range of stability, the designer has more freedom to determine the required step response based on the performance index. As a result, the optimization problem might be used to determine the optimal solution in the future.

Compliance with ethical standards

Disclosure of conflict of interest

No conflict of interest.

References

[1] M. Ahmed, M. F. Hossen, M. E. Hoque, O. Farrok, and M. Mynuddin, "Design and construction of a magnetic levitation system using programmable logic controller," American Journal of Mechanical Engineering, vol. 4, no. 3, pp. 99-107, 2016.

[2] H. Yaghoubi, "The most important maglev applications," Journal of Engineering, vol. 2013, 2013.

[3] N. Pandey, M. Kumar, and P. Tiwari, "Analysis of magnetic levitation and Maglev trains," vol, vol. 3, pp. 108-112, 2016.

[4] M. K. Tummalapalli, S. R. Kommula, B. S. Edara, S. P. Pativada, A. Perabathula, and A. Murty, "MAGNETIC LEVITATION VEHICLE-SUPPORTING GRAVITATIONAL AND ELECTROMAGNETIC PRINCIPLES, THEORIES FOR DESIGNERS."

[5] S. K. Pandey and V. Laxmi, "PID control of magnetic levitation system based on derivative filter," in 2014 Annual International Conference on Emerging Research Areas: Magnetics, Machines and Drives (AICERA/iCMMD), 2014: IEEE, pp. 1-5.

[6] D. Maji, M. Biswas, A. Bhattacharya, G. Sarkar, T. K. Mondal, and I. Dey, "Maglev system modeling and lqr controller design in real time simulation," in 2016 International Conference on Wireless Communications, Signal Processing and Networking (WiSPNET), 2016: IEEE, pp. 1562-1567.

[7] B. Hamed and H. Abu Elreesh, "Design of optimized fuzzy logic controller for magnetic levitation using genetic algorithms," Journal of Information and Communication Technologies, vol. 2, no. 1, 2012.

[8] T.-E. Lee, J.-P. Su, and K.-W. Yu, "Implementation of the state feedback control scheme for a magnetic levitation system," in 2007 2nd IEEE Conference on Industrial Electronics and Applications, 2007: IEEE, pp. 548-553.

[9] M. Hypiusová and A. Kozáková, "Robust PID controller design for the magnetic levitation system: Frequency domain approach," in 2017 21st International Conference on Process Control (PC), 2017: IEEE, pp. 274-279.

[10] I. Ahmad and M. A. Javaid, "Nonlinear model & controller design for magnetic levitation system," Recent advances in signal processing, robotics and automation, pp. 324-328, 2010.

[11] N. Al-Muthairi and M. Zribi, "Sliding mode control of a magnetic levitation system," Mathematical problems in engineering, vol. 2004, no. 2, pp. 93-107, 2004.

[12] X. Shi and Q. Mao, "Research on Control Strategy of Magnetic Levitation Gravity Compensator Based on Lyapunov Stability Criterion," in IOP Conference Series: Materials Science and Engineering, 2018, vol. 452, no. 4: IOP Publishing, p. 042146.

[13] J. G. Ziegler and N. B. Nichols, "Optimum settings for automatic controllers," trans. ASME, vol. 64, no. 11, 1942.

[14] M. Zhuang and D. Atherton, "Automatic tuning of optimum PID controllers," in IEE Proceedings D (Control Theory and Applications), 1993, vol. 140, no. 3: IET, pp. 216-224.

[15] G. Cohen and G. Coon, "Theoretical consideration of retarded control," Transactions of the American Society of Mechanical Engineers, vol. 75, no. 5, pp. 827-834, 1953.

[16] D. W. Pessen, "A new look at PID-controller tuning," 1994.

[17] W. K. Ho, C. C. Hang, and L. S. Cao, "Tuning of PID controllers based on gain and phase margin specifications," Automatica, vol. 31, no. 3, pp. 497-502, 1995.

[18] J. Ackermann, Robust control: Systems with uncertain physical parameters. Springer Science & Business Media, 2012.

[19] N. S. Nise, Control systems engineering. John Wiley & Sons, 2020.

[20] N. Bajcinca, "The method of singular frequencies for robust control design in an affine parameter space," Proc. of MED'01, pp. 100-105, 2001.

[21] B. R. Barmish and E. Jury, "New tools for robustness of linear systems," IEEE Transactions on Automatic Control, vol. 39, no. 12, pp. 2525-2525, 1994.

[22] M. Almobaied, H. S. Al-Nahhal, and K. B. Issa, "Computation Of Stabilizing PID Controllers For Magnetic Levitation System With Parametric Uncertainties," in 2021 International Conference on Electric Power Engineering–Palestine (ICEPE-P), 2021: IEEE, pp. 1-7.

[23] M. J. Khan, D. Khan, S. J. Siddiqi, S. Saleem, and I. Khan, "Design & Control of Magnetic Levitation System ED-4810: Review and Stability Test," 2019.